

Gravitational Wave Opacity from Gauge Field Dark Energy

R. R. Caldwell and C. Devulder

*Department of Physics and Astronomy, Dartmouth College,
6127 Wilder Laboratory, Hanover, New Hampshire 03755 USA*

(Dated: December 3, 2024)

We show that astrophysical gravitational waves can undergo absorption and re-emission when propagating through cosmic gauge field dark energy. A sufficiently strong effect would impact the use of gravitational wave standard sirens to constrain the expansion history of the Universe. We investigate a particular model of dark energy based on a non-Abelian gauge field, and show that at early times it behaves like dark radiation, whereas a novel interaction causes it to drive cosmic acceleration at late times. Joint constraints on the cosmological scenario due to type 1a supernovae, baryon acoustic oscillations, and cosmic microwave background data are presented. We show that standard siren luminosity distances in the redshift range $0.5 \lesssim z \lesssim 1.5$ would suffer at most a 1% absorption.

I. INTRODUCTION

The recent detection of gravitational waves has led to the emergence of gravitational wave astronomy, opening a new vista to astrophysical phenomena. The tantalizing prospect of combining gravitational wave (GW) sources with an electromagnetic counterpart is expected to lead to the development of a new method to constrain the expansion history of the Universe [1, 2]. The GW profile of binary inspirals, for example, is so distinctive that the luminosity distance of the source can be inferred within 1 – 10% uncertainty [3]. Future space-based detectors like LISA [4] are expected to achieve the sensitivity required to make the detection of such “standard sirens” commonplace, extending the reach of GW astronomy to the entire observable Universe in the low frequency range – an unexplored region expected to be rich with both astrophysical and cosmological sources [5, 6].

The luminosity distance inferred from GW standard sirens is susceptible to novel effects that could be within reach of future GW detectors. In particular, we focus on the phenomenon of gravitational wave - gauge field (GWGF) oscillations, in which the amplitude of a GW modulates as it propagates through a cosmic gauge field [7]. In a dark energy model based on a homogeneous non-Abelian gauge field, this effect would result in a distinct imprint on astrophysical GWs. Specifically, GWs couple to wave-like excitations in a background gauge field. At high frequencies relevant for astrophysical sources, the system is akin to a pair of coupled oscillators: as energy exchange occurs between the two oscillators, the GW amplitude weakens and grows continuously, leading to temporal blind spots. An otherwise strong GW would thus arrive at our detectors with a much lower amplitude. To study this effect in a cosmological setting, we begin this article by considering a model of dark energy based on a SU(2) gauge field. While originally introduced in the context of primordial inflation [8], a similar model can also be used to address the present-day cosmic acceleration [9]. We show that the net effect on astrophysical GWs is a redshift-dependent reduction in amplitude which could be within reach of future GW observatories.

The rest of the paper is organized as follows. In Sec. II, we present an illustrative model of GWGF oscillations. In Sec. III, we give an overview of gauge field dark energy, or gauge quintessence, as introduced in [9], and investigate its properties as a dark energy component. We show that, in contrast with most models of dark energy, cosmic acceleration is temporary as the equation of state eventually returns to 1/3 in the future. We constrain the model using observational data from type 1a supernovae, baryon acoustic oscillations and cosmic microwave background experiments. In Sec. IV we return to investigate the interplay between gravitational waves and the gauge field in a dark energy scenario. We present our main result, namely that gauge field dark energy can have a direct impact on the amplitude of astrophysical GWs. Our final discussion is in Sec. V. In Appendix A we explain how to expand the gauge field dark energy to include multiple, disjoint SU(2) subgroups. In Appendix B we show that the same phenomenon could seed a spectrum primordial gravitational waves.

II. A SIMPLE MODEL

To illustrate the effect of a cosmic gauge field on gravitational waves, we begin by considering a gauge field under general relativity:

$$S = \int d^4x \sqrt{-g} \left(\frac{1}{2} M_P^2 R - \frac{1}{4} F_{\alpha\mu\nu} F^{\alpha\mu\nu} + \mathcal{L}_m \right) \quad (1)$$

where we use metric signature $-+++$, M_P is the reduced Planck mass, and \mathcal{L}_m represents any other fields that may be present. We take an $SU(2)$ field

$$F_{\mu\nu}^a = \partial_\mu A_\nu^a - \partial_\nu A_\mu^a - g_Y \epsilon^{abc} A_\mu^b A_\nu^c \quad (2)$$

where g_Y is the Yang-Mills coupling. Greek letters will be used to represent spacetime indices, and Latin letters i, j, \dots are used for spatial indices. To match the symmetries of our cosmological spacetime having line element $ds^2 = a^2(\tau)(-d\tau^2 + d\vec{x}^2)$, the gauge field is taken to be in a flavor-space locked configuration:

$$A_\mu^a = \begin{cases} \phi(t)\delta_\mu^a & \mu = 1, 2, 3 \\ 0 & \mu = 0 \end{cases} \quad (3)$$

i.e. expressed in terms of a triad of mutually orthogonal vectors each associated with a direction of real space, as required to achieve an isotropic and homogeneous configuration.

In this scenario, the gauge field fluctuates in the presence of a GW, in turn setting up travelling waves of its own. For ease of calculation, we consider a gravitational wave propagating in the z -direction:

$$\delta g_{\mu\nu} = a^2 h_{\mu\nu} = a^2 \begin{pmatrix} 0 & 0 & 0 & 0 \\ 0 & h_+ & h_\times & 0 \\ 0 & h_\times & -h_+ & 0 \\ 0 & 0 & 0 & 0 \end{pmatrix}. \quad (4)$$

Similarly, we consider a z -directed gauge field wave

$$\delta A_\mu^a = a y_\mu^a = a \begin{pmatrix} 0 & y_+ & y_\times & 0 \\ 0 & y_\times & -y_+ & 0 \\ 0 & 0 & 0 & 0 \end{pmatrix}. \quad (5)$$

We take the gravitational and gauge field waves to propagate in an expanding spacetime with wavenumber k much greater than both the expansion rate and the gauge field rate of change. In this short-wavelength limit, the equations of motion are identical for both circular polarizations so we drop the subscripts and let $H = aM_p h/\sqrt{2}$ and $Y = \sqrt{2}ay$. The Fourier amplitudes of monochromatic plane wave solutions to the equations of motion are then given by

$$H(\tau) = e^{ib_3\tau} \left[c_0 \cos \omega\tau - \frac{1}{b} \sin b\tau \times ([b_1 + ib_2]c_1 + ib_3c_0) \right] \times e^{-ik\tau} \quad (6)$$

$$Y(\tau) = e^{ib_3\tau} \left[c_1 \cos \omega\tau + \frac{1}{b} \sin b\tau ([b_1 - ib_2]c_0 + ib_3c_1) \right] \times e^{-ik\tau} \quad (7)$$

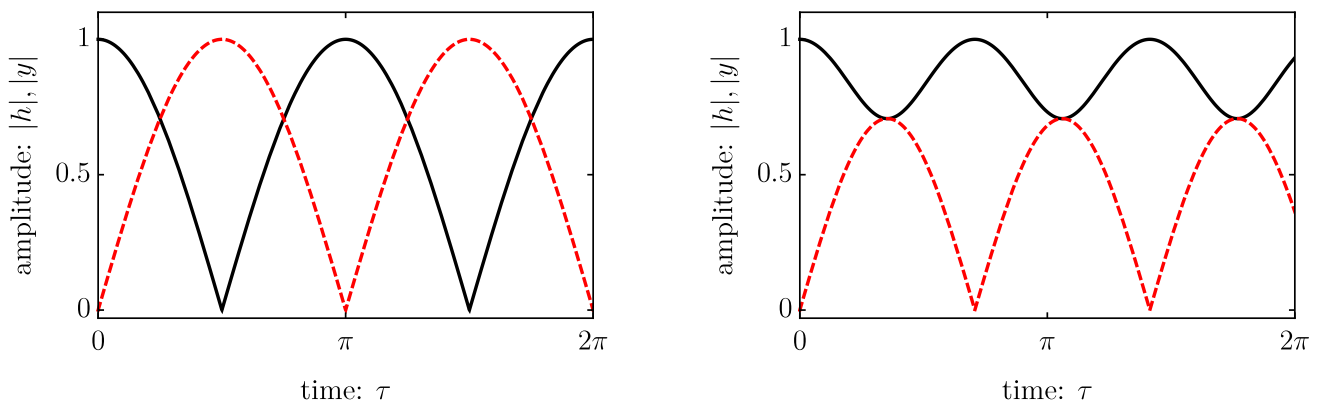


Figure 1: (Left) The oscillations of the gravitational wave amplitude \hbar (black) and gauge field y (dashed). The gravitational wave propagating through a stationary gauge field transforms into a gauge field wave and back again. Complete conversion of GW energy into the gauge field first occurs at $\tau_0 = \tau_{EMIT} + \pi/2$. (Right) Partial absorption of gravitational wave amplitude \hbar by the gauge field y .

where the initial values are $H(0) = c_0, Y(0) = c_1$, the wavenumber k is taken to be large enough such that we can treat the coefficients $b_1 = \phi'/aM_P, b_2 = g_Y\phi^2/aM_P, b_3 = g_Y\phi/2$ as constants, and $b^2 = b_1^2 + b_2^2 + b_3^2$. Note further that we measure conformal time in units of H_0^{-1} and comoving wavenumbers k, b in units of H_0 . In the absence of the gauge field, the gravitational wave solution is simply $H = c_0 e^{ik\tau}$. Hence, the wave amplitude is constant, c_0 , as we have already accounted for redshifting. In the presence of the gauge field, the GW amplitude modulates.

The interaction between gravitational and gauge field waves is revealed by their rms amplitude in the high frequency limit, for which we let $\mathfrak{h}(\tau) = H(\tau)e^{ik\tau}$ and $\mathfrak{y}(\tau) = Y(\tau)e^{ik\tau}$. Fig. 1 shows the oscillations of \mathfrak{h} and \mathfrak{y} for the simple case $b_1 = 1, b_2 = b_3 = 0$. We can use these curves to determine the behavior of a GW burst emitted at a time τ_{EMIT} and observed at a time τ_{OBS} . If the comoving separation is such that $\tau_{OBS} - \tau_{EMIT} = \pi/2$, then the GW will have completely converted into gauge field by the present day. Hence, a gravitational wave observatory on Earth would record no signal. On the other hand, a GW burst from a more distant source whereby $\tau_{OBS} - \tau_{EMIT} = \pi$ would be unaffected.

In general, this energy conversion is only partial. The right panel illustrates the scenario where $b_1 = 0, b_2 = b_3 = 1$, resulting in a smaller fraction of the GW energy being converted into the gauge field. In this case, the maximum conversion occurs when $\tau_0 - \tau_{EMIT} = (2n + 1)\pi/(2\sqrt{2})$ for $n = 1, 2, \dots$. Using standard cosmological parameters to compute conformal times, the most recent maximum conversion ($n = 1$) corresponds to a redshift of emission of $z \simeq 1.7$ ($a/a_0 \simeq 0.4$).

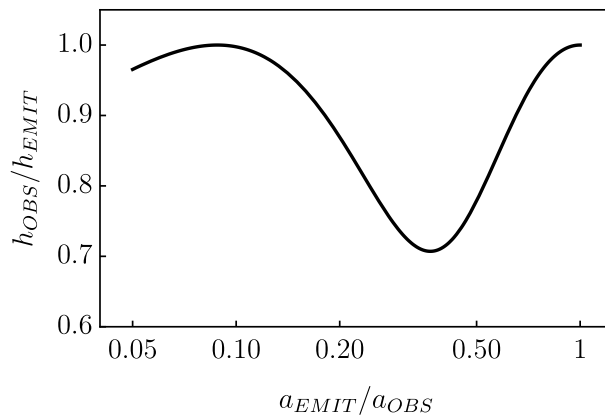


Figure 2: Transmitted gravitational wave amplitude observed today as a function of the scale factor a_{EMIT} at which it is emitted for the case $b_1 = 0, b_2 = b_3 = 1$.

To better illustrate this effect, we have plotted $\mathfrak{h}(\tau_0 - \tau(a_{EMIT}))/\mathfrak{h}_i$ versus scale factor a_{EMIT} in Fig. 2, for the second scenario. This curve represents a sort of visibility function for gravitational waves. To interpret the curve, choose the scale factor at the time of emission, in which case the height of the curve gives the transmitted gravitational wave fraction. For example, a gravitational wave emitted at $a_{EMIT}/a_{OBS} \sim 0.3$ is dimmed by a factor 0.7; a gravitational wave emitted at $a_{EMIT}/a_{OBS} \sim 0.1$ is not dimmed at all. It is easy to see that a standard siren cosmological distance determined from a GW amplitude will be systematically distorted by this effect. In order to make a realistic estimate of the distortion, next, we need to determine the properties of the gauge field in a viable cosmological scenario.

III. GAUGE QUINTESSENCE MODEL

Gauge quintessence is a model of dark energy based on a non-Abelian gauge field [9] which provides a suitable cosmological framework to investigate GWGF interactions. The model consists of an $SU(2)$ gauge field minimally coupled to gravity, as specified by the following action:

$$S = \int d^4x \sqrt{-g} \left(\frac{1}{2} M_P^2 R - \frac{1}{4} F_{a\mu\nu} F^{a\mu\nu} + \frac{\lambda}{M_P^4} (F_{a\mu\nu} \tilde{F}^{a\mu\nu})^2 \right) + S_m(\chi_i, g_{\mu\nu}) \quad (8)$$

where R is the Ricci scalar and S_m is the action for Standard Model particles. The dual field is $\tilde{F}^{a\mu\nu} = \frac{1}{2} \epsilon^{\mu\nu\alpha\beta} F_{\alpha\beta}^a$. The novel λ term is responsible for the negative pressure, leading to cosmic acceleration.

We note that cosmic acceleration under this term can be equivalently described by a system consisting of an axion field with Chern-Simons coupling, as in Chromo-Natural Inflation [10, 11]. In this case, the parameter λ can be related

to the axion mass and the energy scale of the Chern-Simons coupling. However, these models are not equivalent outside of the accelerating regime. The equation of motion for the gauge field follows from varying the action,

$$\nabla^\mu W_{\mu\nu}^a + g_Y f^{abc} A_b^\mu W_{c\mu\nu} = 0, \quad W_{\mu\nu}^a = F_{\mu\nu}^a - 8 \frac{\lambda}{M_P^4} (F\tilde{F})\tilde{F}_{\mu\nu}^a. \quad (9)$$

The stress-energy tensor is

$$T_{\mu\nu} = F_{a\mu\sigma} F_{\nu\tau}^a g^{\sigma\tau} - \frac{1}{4} g_{\mu\nu} F^2 - \frac{\lambda}{M_P^4} g_{\mu\nu} (F\tilde{F})^2. \quad (10)$$

We consider cosmological solutions wherein directions of the internal SU(2) space are aligned with the principle axes of the Cartesian, spatially flat Robertson-Walker spacetime $ds^2 = a^2(\tau)(-d\tau^2 + d\vec{x}^2)$, namely the ansatz known as flavor-space locking of Eqn. (3). For convenience we use prime notation to denote derivatives with respect to τ , and define $\kappa \equiv 96\lambda g_Y^2$. The equation of motion for $\phi(\tau)$ then reads

$$\phi'' + 2g_Y^2 \phi^3 + \frac{\kappa}{a^4 M_P^4} (\phi^4 \phi'' + 2\phi^3 \phi'^2 - 4(a'/a)\phi^4 \phi') = 0. \quad (11)$$

The energy density and pressure are given by

$$\rho = \frac{3}{2} \left(\frac{\phi'^2}{a^4} + g_Y^2 \frac{\phi^4}{a^4} \right) + \frac{3}{2} \frac{\kappa}{M_P^4} \left(\frac{\phi' \phi^2}{a^4} \right)^2 \quad (12)$$

$$p = \frac{1}{2} \left(\frac{\phi'^2}{a^4} + g_Y^2 \frac{\phi^4}{a^4} \right) - \frac{3}{2} \frac{\kappa}{M_P^4} \left(\frac{\phi' \phi^2}{a^4} \right)^2 \quad (13)$$

where the terms involving κ are associated with dark energy, while the remaining contributions account for dark radiation. In this scenario, at early times the energy density is dominated by the κ -independent terms and behaves like a species of dark radiation. The equation of motion $\phi'' + 2g_Y^2 \phi^3 = 0$ is solved by a cosine-like Jacobi elliptic function, $\phi = \phi_i \text{sn}(g_Y \phi_i \tau | -1)$. Although this equation of motion resembles that of a scalar field in a quartic potential, the story is slightly more complicated. Whereas the expression for the energy density may look familiar, the “kinetic” term in the pressure has the wrong sign, such that the κ -independent equation of state is exactly $1/3$. As the field evolves monotonically and the product $\phi' \phi^2$ grows, the κ -dependent term dominates the energy density and pressure so that the equation of state approaches $w \rightarrow -1$, thereby driving cosmic acceleration. In this regime, the solution to the equation of motion is approximately $\phi \propto a(\tau)$ with $a \propto 1/(2\tau_a - \tau)$ for de Sitter-like expansion. However, the equation of motion cannot sustain this solution indefinitely. As a consequence, acceleration is only temporary, for the rapid oscillations of ϕ eventually bring w back up to $1/3$ in the future.

We have also considered the cosmological dynamics in the case that the SU(2) gauge field is replaced by SU(N), where N is sufficiently large to contain \mathcal{N} disjoint SU(2) subgroups. Details are provided in Appendix A. There it is shown that the background equations for the case $\mathcal{N} > 1$ are equivalent to the SU(2) case when the following identifications are made:

$$\phi_N = \frac{1}{\sqrt{\mathcal{N}}} \phi_1, \quad g_N = \sqrt{\mathcal{N}} g_1, \quad \kappa_N = \mathcal{N} \kappa_1. \quad (14)$$

Hence, our study is easily adapted to include larger gauge groups.

A. E and B Solutions

We present the results of the numerical solution of the background equations of motion. Initial values ϕ , ϕ' and parameters g_Y , κ are chosen so that the dark energy equation of state is $w = 1/3$ at early times, deep in the radiation era, and evolves $w \rightarrow -1$ by the present day. Since the dark energy component contributes a non-negligible fraction of the energy budget in the early stages of the matter dominated era, we refer to its contribution as “early dark energy” (EDE). Here we illustrate the case where $\Omega_{EDE} = 0.001$. The YM coupling sets the rate of oscillation of the gauge field, so that in order to enable slow roll-like behavior leading to cosmic acceleration we are compelled to set the coupling constant $\hat{g}_Y \equiv g_Y M_P / H_0$ to order unity. One free parameter remains, κ , which we use to ensure the correct abundance of dark energy at the present day. The photon, neutrino, baryon, and dark matter densities are fixed according to the standard cosmology.

There are two classes of solutions of the gauge field quintessence equation of motion that describe a radiation-dominated fluid which later evolves into dark energy. These are the “B” solutions, in which $g_Y \phi^2 \gg |\phi'|$, and the “E” solutions, in which $g_Y \phi^2 \ll |\phi'|$. These two cases allow for the radiation-like portion of the energy density to dominate over the dark energy term. The nomenclature derives from the similarity with the electric and magnetic field components of the Faraday tensor of electromagnetism. The initial conditions for these two cases can be set as

$$g_Y \phi_i^2 = (2\Omega_{r,0} R \cos^2 \theta)^{1/2} H_0 M_P a_i^2 \quad (15)$$

$$\phi'_i = (2\Omega_{r,0} R \sin^2 \theta)^{1/2} H_0 M_P a_i^2, \quad (16)$$

where $R \equiv \Omega_{EDE}/\Omega_r$ and Ω_r is the fraction of critical density in photons and neutrinos. The above initial conditions ensure that the initial value of $\phi_i'^2 + g_Y^2 \phi_i^4$, appearing in Eqs. (12-13), is a constant. Hence, the gauge field energy density and pressure start out scaling as $1/a^4$ and contribute a fraction Ω_{EDE} of the total energy density, deep in the radiation era.

The B solutions are obtained by setting $\theta \ll 1$. These are the solutions studied in Ref. [9]. In this case, the equation of state is $w = 1/3$ until late times, when it sharply steps down to $w \simeq -1$. The function $w(a) = (1 - 4 \tanh^n(a/a_*))/3$ provides a reasonable fit to the numerical solution, illustrated in Fig. 3, where parameters $n \geq 1$ and a_* depend on parameters R and Ω_M . We note that both signs (\pm) of ϕ_i are considered; there is a slight difference in the solutions, but the broad features are the same. The background evolution of the gauge field quintessence closely resembles that of Λ CDM plus ΔN_ν additional light neutrino species as dark radiation. As such, the model is as viable as one of the most basic extensions of the vanilla Λ CDM cosmology, as explored in Ref. [9]. Current bounds $N_\nu = 3.15 \pm 0.23(1\sigma)$ [12] allow $\Delta N_\nu < 0.33$ and therefore $\Omega_{EDE} < 0.042(1\sigma)$. However, one interesting way in which the background evolution can differ from Λ CDM is suggested by the slight upturn in the equation of state shown in Fig. 3. This upturn presages a sharp spike in w up to $1/3$ in the future before returning back to near -1 . By adjusting g_Y larger or smaller the spike can be moved to earlier times or later times, into the future, respectively. Cosmic acceleration eventually ends, but only after many e-foldings of the accelerated cosmic expansion.

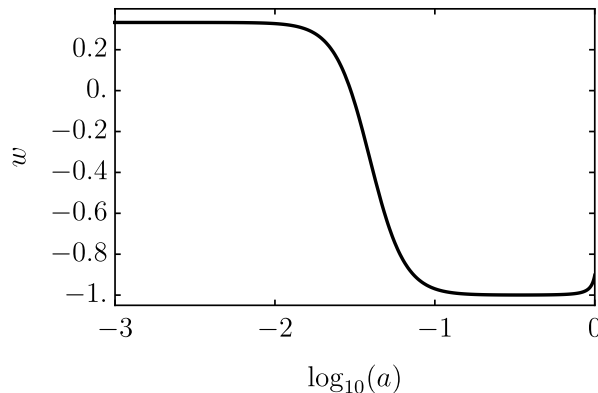


Figure 3: Evolution of the equation of state $w(a)$ under the case of the “B” solution. The time of transition to dark energy behavior is determined by g_Y and Ω_{EDE} . For this model, $\hat{g}_Y = 0.1$, $\kappa = 2.5 \times 10^5$, $R = 0.02$, $\Omega_M = 0.3$ and the present day value of the equation of state is $w_0 = -0.9$. This model uses opposite signs for ϕ_i, ϕ'_i . Using like signs for the initial values ϕ_i, ϕ' , the equation of state curve is identical except with no upturn, such that $w_0 = -0.99$.

The E solutions are obtained by setting $\theta \simeq \pi/2$. The equation of state starts at $w = 1/3$, but it slowly evolves towards -1 as shown in Figs. 4-5, unlike in the case of the B solution. In this case, the cosmic acceleration is temporary: the equation of state eventually returns to $1/3$ as shown in the right panel of Fig. 5, when the gauge field begins to oscillate. This return to radiation domination is in contrast with most freezing models of dark energy where the equation of state decreases toward -1 , and only vaguely resembles most thawing models in which w typically evolves towards matter domination [13]. Fig. 5 shows the evolution of ρ_D, ρ_R and ρ_M , the energy density of gauge quintessence, radiation, and matter, respectively. We note that the crossover shown in the right panel is followed by a reversal of the sign of ρ'_D and ρ'_M , corresponding to the increase of w at later times. In general, increasing \hat{g}_Y or Ω_{EDE} hastens the onset of oscillations of the gauge field, bringing the equation of state to $1/3$ sooner in the future. This behavior, linking the early and late regimes, plays a significant role in determining the observational constraints on this model.

It is interesting to compare the transition from radiation to dark energy behavior with a commonly studied EDE parametrization [14]. Therein, the authors use the fraction of dark energy at early times Ω_{EDE} , its present day value

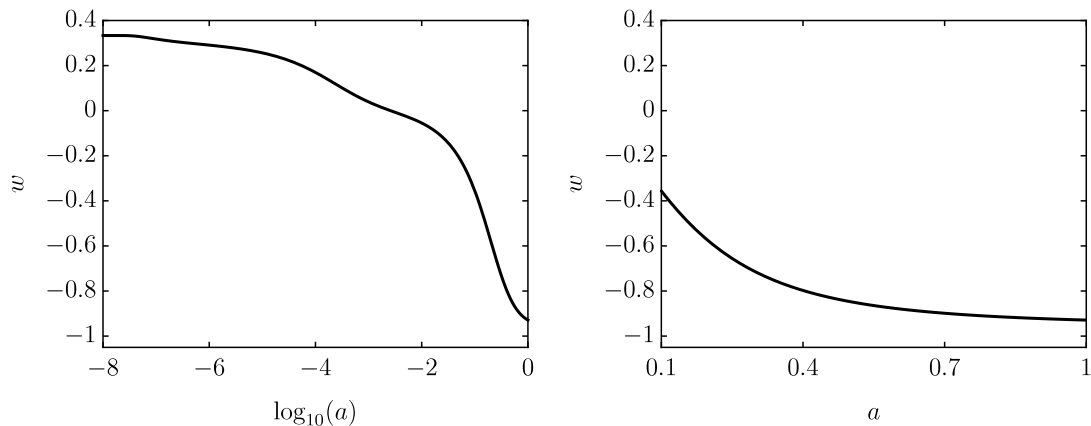


Figure 4: (Left) Evolution of the equation of state $w(a)$. The time of transition to dark energy behavior is determined by \hat{g}_γ and Ω_{EDE} . (Right) Equation of state $w(a)$ from $a = 0.1$ to present time, $a = 1$. Although it resembles the behavior of a cosmological constant, the cosmic acceleration is only temporary.

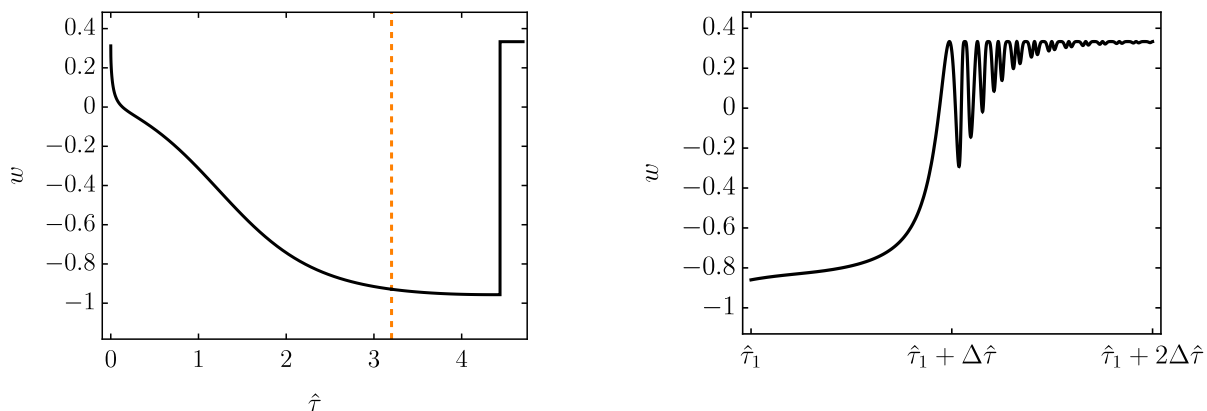


Figure 5: (Left) Equation of state including future behavior, where it asymptotically increases back toward $1/3$. The vertical line at $\hat{\tau} = 3.2$ indicates the present time. (Right) A more careful analysis reveals the oscillating behavior of w as it becomes positive. Here $\hat{\tau}_1 = 4.5813$ and $\Delta\hat{\tau} = 2 \times 10^{-6}$. In this example, the equation of state returns to $w = 1/3$ in approximately 40 Gyrs, at a future redshift $z \sim -0.78$.

Ω_D^0 and w_0 as parameters to derive an analytical expression for the equation of state and abundance of dark energy as a function of a :

$$\Omega_D(a) = \frac{\Omega_D^0 - \Omega_{EDE}(1 - a^{-3w_0})}{\Omega_D^0 + \Omega_M^0 a^{3w_0}} + \Omega_{EDE}(1 - a^{-3w_0}). \quad (17)$$

In this parametrization, the dark component equation of state closely adheres to that of the background until late times. Comparison of the evolution of w and Ω_D in our model with their predictions using $\Omega_{EDE} = 0.003$ is shown in Fig. 7. In contrast, the equation of state of the gauge quintessence model only loosely adheres to that of the background. Moreover, the equation of state arrives near $w \sim -1$ very late, such that this model should be quite distinguishable from Λ CDM.

B. Observational Constraints

We now present constraints on the cosmological parameters of the E solutions of gauge quintessence using a combination of type 1a supernovae (SNe), baryon acoustic oscillations (BAO), and cosmic microwave background (CMB) data. These parameters consist of the present-day abundance, $\Omega_{DE} = 1 - \Omega_M$, the abundance deep in the

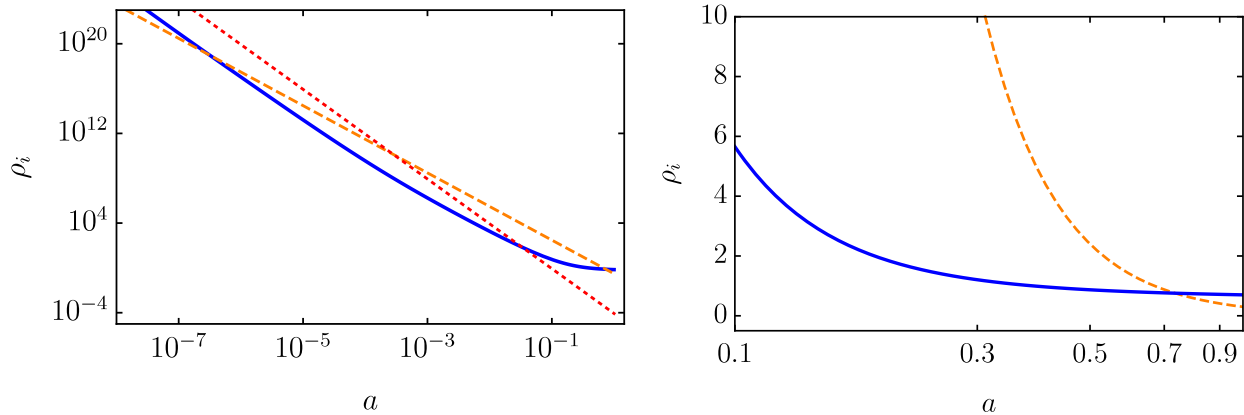


Figure 6: (Left) Energy densities ρ_i in units of the present-day critical energy density vs. scale factor a , showing ρ_D (solid, blue), ρ_R (dotted, red) and ρ_M (dashed, orange). At early times the dark energy component tracks radiation until it reverses direction around $a = 0.001$ and comes to dominate. (Right) Blow up of the cross over between matter and dark energy densities.

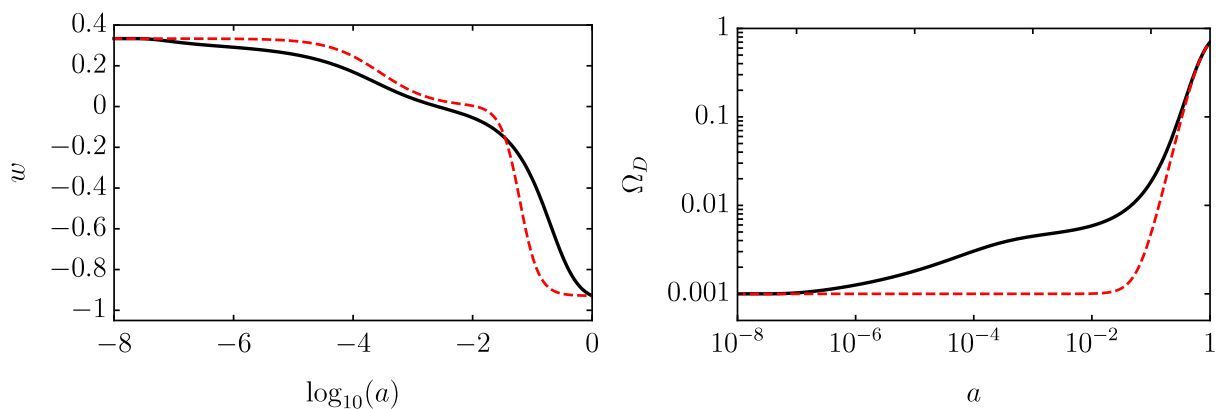


Figure 7: (Left) Equation of state vs. a for the gauge quintessence model (black) and early dark energy analysis (dashed, red). (Right) Evolution of the relative abundance of dark energy for the gauge quintessence model (black) and early dark energy analysis (dashed, red). It can be seen that the relative abundance of dark energy grows more rapidly in our model.

radiation era Ω_{EDE} or alternatively as the abundance at recombination, Ω_{REC} , and finally the Yang-Mills coupling, g_Y . Our purpose is to determine a reasonable range of parameters which we can apply in our study of gravitational wave opacity.

Our constraint analysis proceeds from the following data sets. From SNe [15] we constrain the luminosity distance - redshift relationship, $D_L(z)$. From BAO [16], we constrain the volume-averaged distance $D_V(z)$ and angular diameter distance $D_M(z)$, at several redshifts spanning $z \sim 0.1 - 0.6$, in units of the radius of the sound horizon at decoupling r_d . We use constraints to the baryon density, ω_b , cold dark matter density, ω_c , and the angular diameter distance to the horizon at decoupling from the CMB [17, 18]. This follows the same procedure as in Ref. [16]. We also include the local determination of the Hubble constant [19] which has contributed to the tension in the current data set [20, 21]. We recognize that this procedure is a gross simplification of the influence of gauge field dark energy on cosmological observables. In earlier work, however, we evaluated the effect of scalar and tensor perturbations of a cosmic gauge field as dark radiation on the CMB [22, 23]. There, we found that the dark radiation, present in abundances consistent with the ΔN_ν bounds from Big Bang Nucleosynthesis and CMB recombination physics, did not leave a significant imprint on the CMB anisotropy pattern. We are also ignoring the imprint of the integrated Sachs-Wolfe (ISW) effect on the CMB, which arises from the change to the late-time evolution of the gravitational potentials at the onset of dark-energy domination. However, we note that the other constraints keep the late-time equation of state of the dark energy close to -1 . This means the ISW under these models will not be distinctive relative to the case of Λ CDM. For the time being, we feel justified in this simple analysis, and we expect that parameters within the constraint

boundaries would stand up to a more rigorous analysis.

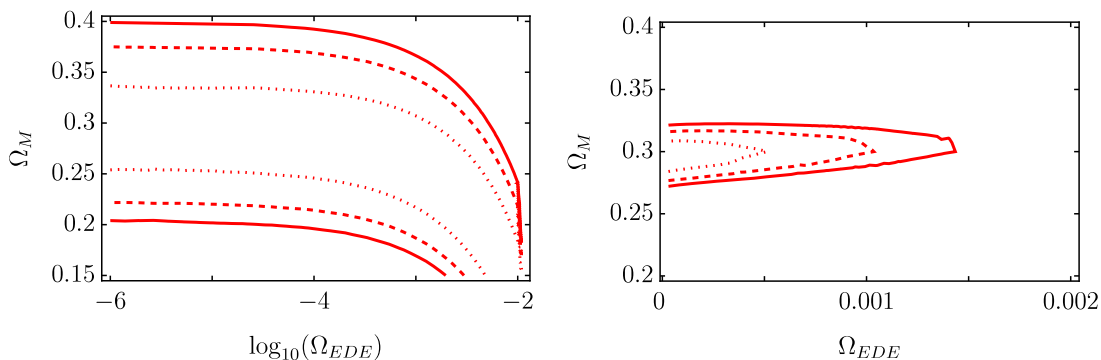


Figure 8: Ω_M vs. Ω_{EDE} contours, for the case $\hat{g}_Y = 1$ are shown due to SNe (left) and BAO and CMB (right). The dotted, dashed and solid lines represent the 1-, 2- and 3- σ contours, respectively.

Contours for various combinations of these data sets are shown in Figs. 8-9. In Fig. 8 we show the supernova luminosity distance - redshift constraint (left) separately from the BAO and CMB constraints (right). Here, we have set the Yang-Mills coupling to $\hat{g}_Y = 1$. For the SNe, the constraint depends only on Ω_M , Ω_{EDE} , and \hat{g}_Y . For the BAO and CMB, we have marginalized over parameters H_0 , ω_b , ω_c . The dotted, dashed and solid lines represent the 1-, 2- and 3- σ contours, respectively. The BAO and CMB clearly give a tighter constraint, but the SNe are important for marking the boundary at the rightmost tip of the constraint region when the two curves are combined. Fig. 9 shows the combined constraints for three values of the Yang-Mills coupling, $\hat{g}_Y = 1, 5, 10$ in red, blue, and green. The two panels show the same constraint regions with the horizontal axis marking either Ω_{EDE} (left) or Ω_{REC} (right). We note that increasing \hat{g}_Y shrinks the constraint region; stronger coupling shortens the duration of the accelerating epoch, but may be compensated for by decreasing the early-time abundance. Further decreasing $\hat{g}_Y < 1$ has the effect of continuing the accelerating era into the future, but otherwise has no effect on the constraint region.

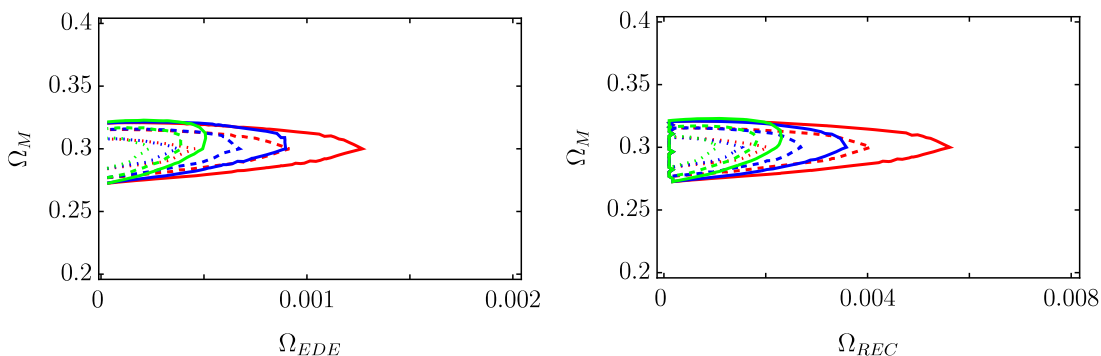


Figure 9: The joint SNe, BAO, and CMB constraints on the Ω_M vs. Ω_{EDE} (left) or Ω_{REC} (right) parameter space for $\hat{g}_Y = 1, 5, 10$ in red, blue, and green.

The results shown here for an $SU(2)$ gauge field can be generalized to $SU(N)$ with N disjoint subgroups, as described in the Appendix. In short, the results for N subgroups, each with $\hat{g}_{Y,N}$, are equivalent to the results for a single $SU(2)$ with $\hat{g}_{Y1} = \hat{g}_{Y,N}/\sqrt{N}$. Hence, increasing the number of fields slightly extends the parameter region to the right, with diminishing effect as \hat{g}_{Y1} approaches unity from above.

IV. MODULATION OF GRAVITATIONAL WAVE AMPLITUDE

We now return to the phenomenon of GWGF oscillations and investigate it in the context of the E and B solutions of the gauge quintessence model as described by the action Eq. (8). We start with a presentation of the gravitational

and gauge field wave equations of motion. We again consider z -directed gravitational and a gauge field waves as given in Eqs. (4-5). To put the action in canonical form, we write

$$h_{+, \times} = \frac{\sqrt{2}}{aM_P} v_{+, \times}, \quad y_{+, \times} = \frac{1}{\sqrt{2}a} u_{+, \times} \quad (18)$$

and furthermore to decouple the equations, we switch to the circular polarization basis

$$\begin{aligned} v_+ &= \frac{1}{\sqrt{2}}(v_L + v_R), & v_\times &= \frac{i}{\sqrt{2}}(v_L - v_R), \\ u_+ &= \frac{1}{\sqrt{2}}(u_L + u_R), & u_\times &= \frac{i}{\sqrt{2}}(u_L - u_R). \end{aligned} \quad (19)$$

The full equations, in terms of the Fourier space amplitudes, are as follows:

$$v''_R + \left[k^2 - \frac{a''}{a} + \frac{2}{a^2 M_P^2} (g_Y^2 \phi^4 - \phi'^2) \right] v_R = \frac{2}{aM_P} [(g_Y \phi - k) g_Y \phi^2 u_R - \phi' u'_R] \quad (20)$$

$$u''_R + \left[k^2 - 2g_Y k \phi - \frac{\kappa}{g_Y M_P^4} (g_Y \phi - k) \left(\frac{\phi^2 \phi'}{a^4} \right)' \right] u_R = \frac{2}{aM_P} \left[a \left(\frac{\phi'}{a} v_R \right)' + (g_Y \phi - k) g_Y \phi^2 v_R \right]. \quad (21)$$

The equations for v_L, u_L are obtained by replacing $k \rightarrow -k$ or $g_Y \rightarrow -g_Y$.

In Appendix A, we generalize these equations to the case where the action features \mathcal{N} disjoint SU(2) subgroups. In this case the energy density and pressure become

$$\rho = \frac{3}{2} \mathcal{N} \left(\frac{\phi'^2}{a^4} + g_Y^2 \frac{\phi^4}{a^4} \right) + \frac{3}{2} \mathcal{N}^2 \frac{\kappa}{M_P^4} \left(\frac{\phi' \phi^2}{a^4} \right)^2, \quad p = \frac{1}{2} \mathcal{N} \left(\frac{\phi'^2}{a^4} + g_Y^2 \frac{\phi^4}{a^4} \right) - \frac{3}{2} \mathcal{N}^2 \frac{\kappa}{M_P^4} \left(\frac{\phi' \phi^2}{a^4} \right)^2 \quad (22)$$

and the equation of motion is

$$\phi'' + 2g_Y^2 \phi^3 + \frac{\kappa}{M_P^4 a^4} \mathcal{N} (\phi^4 \phi'' + 2\phi^3 \phi'^2 - 4(a'/a) \phi^4 \phi') = 0. \quad (23)$$

The gravitational and gauge field wave equations become

$$v''_R + \left[k^2 - \frac{a''}{a} + \frac{2\mathcal{N}}{a^2 M_P^2} (g_Y^2 \phi^4 - \phi'^2) \right] v_R = \sum_{n=1}^{\mathcal{N}} \frac{2}{aM_P} [(g_Y \phi - k) g_Y \phi^2 u_{Rn} - \phi' u'_{Rn}] \quad (24)$$

$$u''_{Rn} + \left[k^2 - 2g_Y k \phi - \frac{\kappa}{g_Y M_P^4} \mathcal{N} (g_Y \phi - k) \left(\frac{\phi^2 \phi'}{a^4} \right)' \right] u_{Rn} = \frac{2}{aM_P} \left[a \left(\frac{\phi'}{a} v_R \right)' + (g_Y \phi - k) g_Y \phi^2 v_R \right]. \quad (25)$$

As derived in Ref. [7], we obtain the equations of motion in the high-frequency limit by making the ansatz $v = \hbar e^{-ik\tau}$ and $u_n = \mathbf{y}_n e^{-ik\tau}$, whereupon the amplitudes evolve as

$$\hbar'_R = -\frac{1}{aM_P} \sum_n (\phi' + ig_Y \phi^2) \mathbf{y}_{Rn}, \quad \mathbf{y}'_{Rn} = \frac{1}{aM_P} (\phi' - ig_Y \phi^2) \hbar_R + ig_Y \phi \mathbf{y}_{Rn} - \frac{i\kappa \mathcal{N}}{2g_Y M_P^4} (\phi^2 \phi' / a^4)' \mathbf{y}_{Rn}. \quad (26)$$

The equations for the left-handed polarization are obtained by taking $g_Y \rightarrow -g_Y$, which is equivalent to taking the complex conjugate of the equations of motion. Hence, the results in terms of the wave amplitude are the same for either chirality.

The background equations for the case $\mathcal{N} > 1$ are equivalent to the SU(2) case when the following identifications are made:

$$\phi_{\mathcal{N}} = \frac{1}{\sqrt{\mathcal{N}}} \phi_1, \quad g_{\mathcal{N}} = \sqrt{\mathcal{N}} g_1, \quad \kappa_{\mathcal{N}} = \mathcal{N} \kappa_1. \quad (27)$$

Furthermore, when all the gauge field waves behave identically, such that $\mathbf{y}_1 = \mathbf{y}_2 \dots$, then we define $\mathbf{y}_{\mathcal{N}} \equiv \mathcal{N}^{-1} \sum \mathbf{y}_n$, such that if we rescale

$$\mathbf{y}_{\mathcal{N}} = \frac{1}{\sqrt{\mathcal{N}}} \mathbf{y}_1 \quad (28)$$

then the high frequency equations of motion are equivalent to the $SU(2)$ case.

We solve the system of equations (26) describing high frequency gravitational and tensor gauge field waves. We use boundary conditions $\dot{h} = 1$ and $\mathbf{y} = 0$ to determine the gravitational wave opacity due to the gauge field. We can also see the coefficients referred to earlier as $b_1 = \phi'/aM_P$, $b_2 = g_Y\phi^2/aM_P$, and $b_3 = g_Y\phi$. Inspecting Eqs. (26), we determine that these coefficients must be non-negligible relative to a'/a in order for the gauge field wave to grow and thereby damp the gravitational wave.

As an aside, we note that the phenomena of gravitational wave - gauge field oscillations leads to interesting effects at long wavelengths, too. In Appendix B we show how a spectrum of long wavelength tensor fluctuations of the gauge field can seed a similar spectrum of gravitational waves.

A. Gravitational Wave Opacity under B Solutions

The high-frequency gravitational wave transmission is nearly 100%, meaning the opacity is nearly zero, in the presence of the B solutions of the gauge quintessence equations of motion. An example is shown in Fig. 10. The reason for the weak effect is that the dark energy equation of state $w \approx -1$ suppresses the growth of fluctuations in the gauge field, thereby leaving the gravitational waves free to propagate. All the coefficients b_i , as well as the new term $\kappa(\phi^2\phi'/a^4)/g_Y M_P^4$ in Eqs (26), are sufficiently small that the gauge field wave y is unexcited and therefore h is undisturbed.

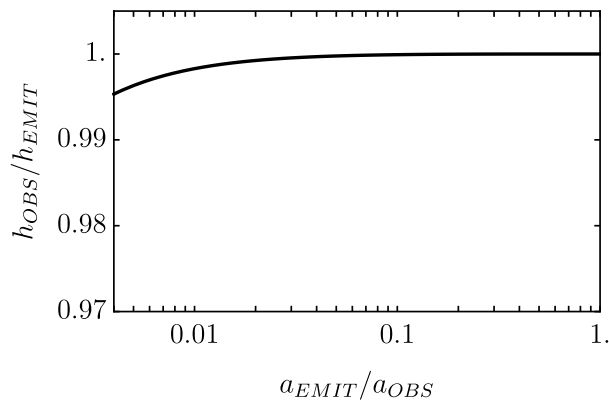


Figure 10: The high frequency gravitational wave transmission amplitude is shown for the case of a sample B solution, also illustrated in Fig. 3. In this case, as with all B solutions, the effect of the gauge field is negligible and the transmission is nearly 100%. Only for GWs that originate at $z \gtrsim 250$ is there $\sim 0.5\%$ suppression.

B. Gravitational Wave Opacity under E Mode Solutions

We naively expect the gravitational wave transmission to decrease by $\sim 1 - 10\%$ in the presence of E solutions. It is easy to find numerical examples of models that are superficially consistent with data – e.g. negative equation of state at present, abundant in the radiation era, consistent with the bound on ΔN_ν – which lead to a significant suppression of gravitational wave amplitude. However, a careful analysis of observational constraints leads to a different story. The high-frequency gravitational wave opacity dips at most by $\sim 1\%$ in the presence of the E solutions of the gauge quintessence equations of motion that are also compatible with the observational constraints. The effect, illustrated in Fig. 11, is peaked at $z = 1$. In the absence of the resonant conversion effect, the amplitude should be constant as we have already removed the redshifting of the wave energy. For comparison, we also show the opacity for a model with Ω_{EDE} that exceeds the observational bounds. The effect in the case of the E solutions is greater than for the B solutions because the coefficients b_i are larger; the background field is not frozen but has been evolving since early times. However, because the equation of state only slowly interpolates between $1/3$ and -1 early in the matter era, the dark energy density grows anomalously large. Hence, a tight constraint on Ω_{EDE} keeps compatibility with the angular diameter distance to the CMB but also dilutes the effect on gravitational waves.

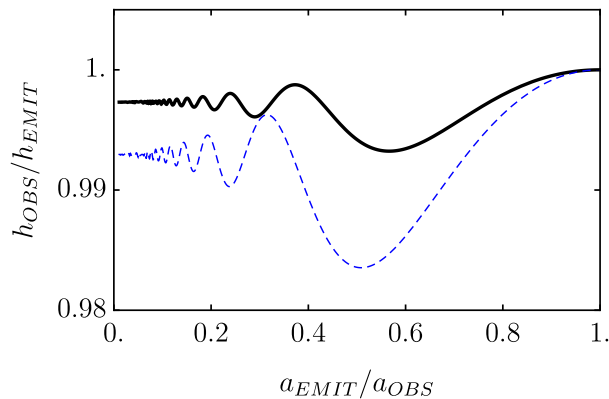


Figure 11: The high frequency gravitational wave transmission amplitude is shown for the case of a sample E solution. The solid (black) curve is for a model with $\Omega_M = 0.3$, $\hat{g}_Y = 1$ and $\Omega_{EDE} = 0.0013$, lying on the boundary of the 2σ contour, illustrated in Fig. 9. The effect is small, with less than 1% dimming of standard sirens emitted near $z = 1$. For comparison, the dashed (blue) curve shows the opacity for a model with $\Omega_M = 0.3$, $\hat{g}_Y = 1$, and $\Omega_{EDE} = 0.003$, which is incompatible with the observational constraints.

V. DISCUSSION

In this work we have investigated a model of gauge field dark energy in which GWs are absorbed and re-emitted by the gauge field. This resonant conversion of energy translates into a distinct modulation pattern on the GW amplitude, which we describe as a redshift dependent opacity. Such an effect could have implications for the use of standard sirens to chart the cosmic expansion history. In the event the GW source can be coupled with an electromagnetic counterpart, it is expected that its luminosity distance can be inferred within 1 – 10% uncertainty [3], which in turn can be used to constrain H_0 at the level of 0.5% in the most favorable scenarios [6].

The dark energy model, gauge quintessence, features an equation of state $w = 1/3$ at early times, but which evolves to $w \simeq -1$ by the present day. We have shown that there are two broad classes of gauge field evolution that realize these features, labelled B- and E-solutions. Whereas the equation of state under the B solution evolves sharply from $w = 1/3$ to $w = -1$, the evolution under the E solution is softer. The consequences are twofold. First, the field evolution in the late universe under the E solution is greater than the under the B solution. This means that the rate of gravitational wave - gauge field oscillation is greater under E than B. Second, the softer evolution of w under the E solutions means the energy density during the matter era is greater than under B. By evaluating the observational constraints based on SNe, CMB and BAO data, we have been able to determine the viable range of dark energy parameters. We used these results to study the gravitational wave opacity in these models.

Despite simple expectations that the opacity could have a $\sim 1 - 10\%$ effect on gravitational wave amplitudes, we find that for realistic models the dimming is much smaller. For E solutions, the dimming is at most 1% for sources emitted near redshift 1.5. For B solutions, the dimming is negligible. With regard to LISA, systematic uncertainty in siren luminosity distance [5] is already expected to be $\sim 5\%$ due to weak lensing alone [2]. In comparison, the gravitational effect investigated in this paper is much smaller. This speculative form of dark energy will not affect measurements of standard sirens.

Acknowledgments

We thank Eric Linder for useful comments. This work is supported in part by DOE grant DE-SC0010386.

Appendix A: Multiple Gauge Field Quintessence

By taking advantage of the fact that multiple $SU(2)$ subgroups may be embedded in a larger $SU(N)$ group, the gauge quintessence model can be generalized to include an arbitrary number of gauge-fields. In this section, we give an overview of the mathematical procedure behind this approach, effectively introducing an extra degree of freedom \mathcal{N} corresponding to the number of fields in the model.

In the single field case, the requirement of Eqn. (3) ensures that the flavor components of A_μ match the generators of the SU(2) group that make up the canonical basis of its algebra – namely, the Pauli matrices. Specifically, each Pauli matrix σ_i is uniquely associated with one of the vectors A_μ , where $\mu \neq 0$, so that $A_i^i = \phi(t)$. Note that the choice $\mu = i$ is not essential to guarantee isotropy as the resulting equations of motion remain unchanged in all six possible alignments.

In fact, rewriting equation Eqn. (2),

$$F_{\mu\nu}^a = \partial_\mu A_\nu^a - \partial_\nu A_\mu^a - g_Y f_{bc}^a A_\mu^b A_\nu^c \quad (\text{A1})$$

we note that the theory remains unchanged for different SU(N) gauges, provided A_μ^a is constructed according to one of the $N^2 - 1$ dimensional bases of $\mathfrak{su}(2)$ – the algebra of SU(2). Thus, while a now runs from $1, \dots, N^2 - 1$, only those components of A^μ which are mapped to an SU(2) subgroup of SU(N) will contribute to the field strength, and will do so identically to the $N = 2$ case.

The larger dimensionality, however, gives more freedom in choosing a particular basis of generators, since we are no longer limited to the Pauli matrices but may instead pick another basis to populate our gauge field. For example, with SU(3), one may define A_μ^a as either one of the following two matrices (omitting the time component):

$$A_i^a = \phi(t) \begin{pmatrix} 1 & 0 & 0 \\ 0 & 1 & 0 \\ 0 & 0 & 1 \\ 0 & 0 & 0 \\ 0 & 0 & 0 \\ 0 & 0 & 0 \\ 0 & 0 & 0 \end{pmatrix}, \quad A_i^a = \phi(t) \begin{pmatrix} 0 & 0 & 0 \\ 0 & 0 & 0 \\ 0 & 0 & -\frac{1}{2} \\ 0 & 0 & 0 \\ 0 & 0 & 0 \\ 1 & 0 & 0 \\ 0 & 1 & 0 \\ 0 & 0 & \frac{\sqrt{3}}{2} \end{pmatrix} \quad (\text{A2})$$

The second arrangement corresponds to the following basis

$$\{\lambda_6, \lambda_7, \frac{1}{2}(-\lambda_3 + \sqrt{3}\lambda_8)\} \quad (\text{A3})$$

where the λ_i denote the Gell-Mann matrices. One will also recognize it as the basis used in constructing one of the standard SU(3) ladder operators:

$$U_\pm = \frac{1}{2}(\lambda_6 \pm i\lambda_7), \quad U_z = \frac{1}{2}(-\lambda_3 + \sqrt{3}\lambda_8) \quad (\text{A4})$$

Since a basis for $\mathfrak{su}(3)$ can be defined so as to carry over the Pauli matrices in the form of 2×2 block matrices embedded in 3×3 generators, we effectively end up with two SU(2) subgroups to choose from. Though more combinations of generators obeying the SU(2) commutation relations can be found, only those corresponding to the $N - 1$ basis elements of the Cartan subalgebra will here be considered, and henceforth referred to as independent.

In order to include more than one field in our action, the gauge field is taken as the sum of two or more subcomponents, each populated according to its own corresponding SU(2) subgroup:

$$A_\mu^a = A_\mu^a(1) + A_\mu^a(2) + A_\mu^a(3) + \dots \quad (\text{A5})$$

where each individual $A_\mu^a(i)$ is labeled according to which independent SU(2) subgroup it corresponds to. In SU(4), there are 3 such subgroups, namely

$$S_1 = \{\lambda_1, \lambda_2, \lambda_3\} \quad (\text{A6})$$

$$S_2 = \{\lambda_6, \lambda_7, \frac{1}{2}(-\lambda_3 + \sqrt{3}\lambda_8)\} \quad (\text{A7})$$

$$S_3 = \{\lambda_{13}, \lambda_{14}, \frac{1}{3}(-\sqrt{3}\lambda_8 + \sqrt{6}\lambda_{15})\} \quad (\text{A8})$$

where each generator making up the 15-dimensional basis of $\mathfrak{su}(4)$ is now a 4×4 matrix.

Furthermore, in building A_μ^a , only those $A_\mu^a(i)$ whose corresponding bases S_i are disjoint may be combined, or else isotropy will be spoiled in the direction of overlap. For example, an SU(3) gauge-field built out of $A_\mu^a(1)$ and $A_\mu^a(2)$ will result in an anisotropic stress-energy tensor as the pressure component in the z direction will differ from the other

two – a direct consequence of the fact that $S_1 \cap S_2 = \lambda_3$. Hence, for a two-field configuration, we consider the SU(4) gauge, where

$$A_\mu^a = A_\mu^a(1) + A_\mu^a(3) \quad (\text{A9})$$

This puts a further restriction on the maximum number of independent, non-overlapping gauge fields \mathcal{N} one can form out for each of the $N - 1$ Cartan elements in SU(N), and it can easily be shown that \mathcal{N} is the greatest integer such that $\mathcal{N} \leq N/2$. Therefore, our model can accommodate up to two fields in an SU(4) and SU(5) gauge, three in an SU(6) and SU(7) gauge, etc.

This procedure can be generalized to any SU(N) group, and thus any number of field \mathcal{N} . In order to devise a basis for $\mathfrak{su}(N)$, we seek $N^2 - 1$ linearly independent traceless Hermitian matrices. If we let M_{mn} denote the $N \times N$ matrix with 1 in the m^{th} row and n^{th} column and zeroes elsewhere, these matrices may be constructed as follows:

$$\begin{aligned} M_{nm} + M_{mn} & \quad (1 \leq m < n \leq N) \\ iM_{nm} - iM_{mn} & \quad (1 \leq m < n \leq N) \\ (I - NM_{nn})/A_n & \quad (n \leq N) \end{aligned} \quad (\text{A10})$$

where I is the $N \times N$ identity matrix and

$$A_N \equiv \sqrt{\frac{(N-1) + (N-1)^2}{2}} \quad (\text{A11})$$

is the normalization factor. The extra SU(2) subgroup can then be constructed similarly by considering the ladder operator corresponding to the extra Cartan element given by $(I - NM_{NN})/\sqrt{A_N}$, and which in general can be associated with the following basis:

$$S_{N-1} = \left\{ \lambda_{N^2-3}, \lambda_{N^2-2}, \frac{1}{N-1} (A_N \lambda_{N^2-1} - A_{N-1} \lambda_{(N-1)^2-1}) \right\} \quad (\text{A12})$$

where generators are labelled according to the ordering prescribed by Eqn. (A10).

In the case of \mathcal{N} disjoint SU(2) subgroups, of which \mathcal{N}_R are right handed and \mathcal{N}_L are left handed, the energy density and pressure become

$$\rho = \frac{3}{2} \mathcal{N} \left(\frac{\phi'^2}{a^4} + g_Y^2 \frac{\phi^4}{a^4} \right) + \frac{3}{2} \Delta \mathcal{N}^2 \frac{\kappa}{M_P^4} \left(\frac{\phi' \phi^2}{a^4} \right)^2, \quad p = \frac{1}{2} \mathcal{N} \left(\frac{\phi'^2}{a^4} + g_Y^2 \frac{\phi^4}{a^4} \right) - \frac{3}{2} \Delta \mathcal{N}^2 \frac{\kappa}{M_P^4} \left(\frac{\phi' \phi^2}{a^4} \right)^2 \quad (\text{A13})$$

where $\Delta \mathcal{N} = \mathcal{N}_R - \mathcal{N}_L$. The equation of motion is

$$\phi'' + 2g_Y^2 \phi^3 + \frac{\kappa}{a^4 M_P^4} \frac{\Delta \mathcal{N}^2}{\mathcal{N}} (\phi^4 \phi'' + 2\phi^3 \phi'^2 - 4(a'/a) \phi^4 \phi') = 0. \quad (\text{A14})$$

The gravitational wave equation becomes

$$\begin{aligned} v_R'' + \left[k^2 - \frac{a''}{a} + \frac{2\mathcal{N}}{a^2 M_P^2} (g_Y^2 \phi^4 - \phi'^2) \right] v_R &= \sum_{n=1}^{\mathcal{N}_R} \frac{2}{a M_P} [(g_Y \phi - k) g_Y \phi^2 u_{Rn} - \phi' u'_{Rn}] \\ &+ \sum_{n=\mathcal{N}_R+1}^{\mathcal{N}} \frac{2}{a M_P} [(g_Y \phi + k) g_Y \phi^2 u_{Rn} - \phi' u'_{Rn}]. \end{aligned} \quad (\text{A15})$$

For the gauge field waves with $n \in [1, \mathcal{N}_R]$, the equation of motion is

$$u_{Rn}'' + \left[k^2 - 2g_Y k \phi - \frac{\kappa \Delta \mathcal{N}}{g_Y M_P^4} (g_Y \phi - k) \left(\frac{\phi^2 \phi'}{a^4} \right)' \right] u_{Rn} = \frac{2}{a M_P} \left[a \left(\frac{\phi'}{a} v_R \right)' + (g_Y \phi - k) g_Y \phi^2 v_R \right]. \quad (\text{A16})$$

For the gauge field waves with $n \in [\mathcal{N}_R + 1, \mathcal{N}]$, the equation of motion is

$$u_{Rn}'' + \left[k^2 + 2g_Y k \phi + \frac{\kappa \Delta \mathcal{N}}{g_Y M_P^4} (g_Y \phi + k) \left(\frac{\phi^2 \phi'}{a^4} \right)' \right] u_{Rn} = \frac{2}{a M_P} \left[a \left(\frac{\phi'}{a} v_R \right)' + (g_Y \phi + k) g_Y \phi^2 v_R \right]. \quad (\text{A17})$$

These latter equations are obtained from the former by replacing $g_Y \rightarrow -g_Y$, recognizing that this also swaps $\Delta\mathcal{N} \rightarrow -\Delta\mathcal{N}$. The high-frequency evolution equations similarly become

$$\dot{h}'_R = -\frac{1}{aM_P} \left(\sum_{n=1}^{\mathcal{N}_R} (\phi' + ig_Y \phi^2) \mathbf{y}_{Rn} + \sum_{n=\mathcal{N}_R+1}^{\mathcal{N}} (\phi' - ig_Y \phi^2) \mathbf{y}_{Rn} \right), \quad (\text{A18})$$

$$\mathbf{y}'_{Rn} = \frac{1}{aM_P} (\phi' - ig_Y \phi^2) \dot{h}_R + ig_Y \phi \mathbf{y}_{Rn} - \frac{i\kappa \Delta\mathcal{N}}{2g_Y M_P^4} (\phi^2 \phi' / a^4)' \mathbf{y}_{Rn}, \quad n \in [1, \mathcal{N}_R] \quad (\text{A19})$$

$$\mathbf{y}'_{Rn} = \frac{1}{aM_P} (\phi' + ig_Y \phi^2) \dot{h}_R - ig_Y \phi \mathbf{y}_{Rn} - \frac{i\kappa \Delta\mathcal{N}}{2g_Y M_P^4} (\phi^2 \phi' / a^4)' \mathbf{y}_{Rn}, \quad n \in [\mathcal{N}_R + 1, \mathcal{N}]. \quad (\text{A20})$$

The equations for the left-handed polarization are obtained by taking $g_Y \rightarrow -g_Y$.

Appendix B: Gravitational waves generated from gauge field perturbations

We have focused throughout this article on the behavior of gravitational waves in the presence of an initially smooth gauge field. Here we turn the situation around to investigate the interplay between tensor fluctuations of the gauge field and an initially smooth gravitational field. In particular, we consider the production of gravitational waves in the presence of a superhorizon gauge field wave. For simplicity, the theory is given by following action

$$S = \int d^4x \sqrt{-g} \left(\frac{1}{2} M_P^2 R - \frac{1}{4} F_{a\mu\nu} F^{a\mu\nu} + \mathcal{L}_m \right) \quad (\text{B1})$$

All other fields, matter and radiation, are described by \mathcal{L}_m . In this scenario, the equation of motion for ϕ is then given by

$$\phi'' + 2g_Y^2 \phi^3 = 0 \quad (\text{B2})$$

which is solved analytically in terms of a Jacobi elliptic function

$$\phi = c_1 \text{sn}(c_1(\tau - \tau_i) + c_2 | -1) / g_Y \quad (\text{B3})$$

where τ_i is some initial time. The constants c_1 and c_2 are determined at the initial time, which we will take to be deep in the radiation era, and may be expressed in terms of the fraction of critical density in the form of the gauge field, Ω_{EDE} , plus a mixing angle θ that describes the apportionment of energy between the gauge electric and magnetic fields. Hence, we set

$$\begin{aligned} \phi'_i &= a_i^2 H_i M_P \sqrt{2\Omega_{EDE}} \sin \theta \\ \phi^2_i &= a_i^2 H_i M_P \sqrt{2\Omega_{EDE}} \cos \theta / g_Y \end{aligned} \quad (\text{B4})$$

and allow $\theta \in [0, \pi/2]$. We determine that $c_1 = (2\Omega_{EDE})^{1/4} (g_Y H_i M_P)^{1/2} a_i$ and $c_2 = F(\text{csc}^{-1}(\sqrt{\sec \theta}) | -1)$ where F is an elliptic integral of the first kind. Subsequently, we may write

$$\phi = c_1 \psi(x) / g_Y, \quad \phi' = c_1^2 \psi'(x) / g_Y \quad (\text{B5})$$

where $\psi(x) = \text{sn}(x | -1)$ and $d\psi(x) = \text{cn}(x | -1) \text{dn}(x | -1)$ and $x = c_1(\tau - \tau_i) + c_2$.

We again consider tensor fluctuations of the gauge field, and the resulting gravitational waves, as given by Eqs. (4-5). We insert these into the action of Eq. (B1) and expand to second order. In the long-wavelength limit, the equations of motion are identical for both left- and right-circular polarizations so we drop the subscripts, whereby variation with respect to h and y yields

$$y'' + 2\frac{a'}{a}y' + \frac{a''}{a}y = -\frac{2}{aM_P} [g_Y^2 \phi^3 h - \phi' h'] \quad (\text{B6})$$

$$h'' + 2\frac{a'}{a}h' + \frac{2}{a^2 M_P^2} (g_Y^2 \phi^4 - \phi'^2) h = -\frac{2}{a^2 M_P} \left[-g_Y^2 \phi^3 y + \frac{a'}{a} \phi' y + \phi' y' \right]. \quad (\text{B7})$$

This system of equations can be put in dimensionless form, defining $\tilde{\tau} = a_i H_i \tau$ and $\tilde{g}_Y = g_Y \sqrt{2\Omega_{YM}} M_P / H_i$ and H_i is the Hubble constant at the starting time, so that $\tilde{\tau}_i = 1$:

$$\frac{d^2 y}{d\tilde{\tau}^2} + \frac{2}{\tilde{\tau}} \frac{dy}{d\tilde{\tau}} = -2 \frac{\sqrt{2\Omega_{EDE}}}{\tilde{\tau}} \left(\sqrt{\tilde{g}_Y} \psi^3 h - d\psi \frac{dh}{d\tilde{\tau}} \right) \quad (\text{B8})$$

$$\frac{d^2 h}{d\tilde{\tau}^2} + \frac{2}{\tilde{\tau}} \frac{dh}{d\tilde{\tau}} + \frac{4\Omega_{EDE}}{\tilde{\tau}^2} (\psi^4 - d\psi^2) h = -2 \frac{\sqrt{2\Omega_{EDE}}}{\tilde{\tau}} \left(-\sqrt{\tilde{g}_Y} \psi^3 y + d\psi \frac{y}{\tilde{\tau}} + d\psi \frac{dy}{d\tilde{\tau}} \right) \quad (\text{B9})$$

The argument of the elliptic Jacobi functions is $\psi = \psi(x[\tilde{\tau}])$ where $x = \sqrt{\tilde{g}_Y}(\tilde{\tau} - \tilde{\tau}_i) + c_2$.

In previous work we considered the behavior of a primordial gravitational wave spectrum in the presence of an undisturbed flavor-space locked gauge field [23]. Here, we consider the behavior of the system subject to the initial conditions in which there is no gravitational wave, $h_i = h'_i = 0$, but there is a frozen, superhorizon gauge field wave, $y_i \neq 0, y'_i = 0$.

We consider first the case of color electrodynamics, which corresponds to setting $g_Y \rightarrow 0$ in Eqs. (B6-B7) or $\psi \rightarrow 0$ and $d\psi \rightarrow 1$ in Eqs. (B8-B9). The solutions are

$$\begin{aligned} h &= y_i \frac{\sqrt{2}}{\alpha} \left[\sqrt{\frac{1+\alpha}{1-\alpha}} \tilde{\tau}^{-\frac{1}{2} + \frac{\alpha}{2}} - \sqrt{\frac{1-\alpha}{1+\alpha}} \tilde{\tau}^{-\frac{1}{2} - \frac{\alpha}{2}} - \frac{2\alpha}{\sqrt{1-\alpha^2}} \right] \\ y &= y_i \left[-1 + \frac{2}{\tilde{\tau}} - \frac{2}{\alpha} \tilde{\tau}^{-\frac{1}{2} - \frac{\alpha}{2}} + \frac{2}{\alpha} \tilde{\tau}^{-\frac{1}{2} + \frac{\alpha}{2}} \right] \end{aligned} \quad (\text{B10})$$

where $\alpha = 1 - 16\Omega_{EDE}$. For $\Omega_{EDE} \ll 1$, the gravitational wave amplitude asymptotes in the future to $-y_i/(2\sqrt{\Omega_{EDE}})$. In this same limit, the gauge field amplitude swaps from $+y_i$ to $-y_i$.

In the case of SU(2), we integrate Eqs. B8-B9, subject to the same initial conditions $h_i = h'_i = 0$, and $y_i \neq 0, y'_i = 0$. We find that the gravitational wave amplitude grows rapidly and asymptotes to a constant value at time $\tilde{\tau} \gg P/\sqrt{\tilde{g}_{YM}}$ where $P = \Gamma(1/4)^2/\sqrt{2\pi}$ is the oscillation period of the Jacobi elliptic functions, while the final amplitude depends on the parameters g_Y and Ω_{YM} . A sample case is shown in Fig. 12, which illustrates our main result: a super-horizon gauge field wave creates a super-horizon gravitational wave. We leave for future investigations how this phenomenon may feature in a cosmological scenario.

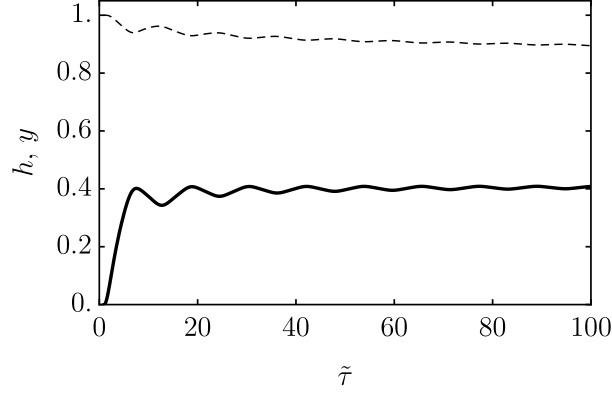


Figure 12: A super-horizon gauge field wave creates a super-horizon gravitational wave. The gravitational wave amplitude h (solid) starts at zero but quickly asymptotes to a constant value. The gauge field wave y (dashed) starts at a constant value and decays. In this example we have set $\Omega_{EDE} = 0.02$ and $\tilde{g}_Y = 1$. We have chosen initial conditions for the background gauge field $\psi_i = 1$ and $d\psi_i = 0$.

-
- [1] B. F. Schutz, *Nature* **323**, 310 (1986). doi:10.1038/323310a0
 - [2] D. E. Holz and S. A. Hughes, *Astrophys. J.* **629**, 15 (2005) doi:10.1086/431341 [[astro-ph/0504616](#)].
 - [3] S. A. Hughes, *Mon. Not. Roy. Astron. Soc.* **331**, 805 (2002) doi:10.1046/j.1365-8711.2002.05247.x [[astro-ph/0108483](#)].
 - [4] H. Audley *et al.*, [arXiv:1702.00786](#) [astro-ph.IM].
 - [5] N. Tamanini, C. Caprini, E. Barausse, A. Sesana, A. Klein and A. Petiteau, *JCAP* **1604**, no. 04, 002 (2016) doi:10.1088/1475-7516/2016/04/002 [[arXiv:1601.07112](#) [astro-ph.CO]].
 - [6] C. Caprini and N. Tamanini, [arXiv:1607.08755](#) [astro-ph.CO].
 - [7] R. R. Caldwell, C. Devulder and N. A. Maksimova, [arXiv:1604.08939](#) [gr-qc].
 - [8] A. Maleknejad and M. M. Sheikh-Jabbari, *Phys. Lett. B* **723**, 224 (2013) doi:10.1016/j.physletb.2013.05.001 [[arXiv:1102.1513](#) [hep-ph]].
 - [9] A. Mehrabi, A. Maleknejad and V. Kamali, *Astrophys. Space Sci.* **362**, no. 3, 53 (2017) doi:10.1007/s10509-017-3033-z [[arXiv:1510.00838](#) [astro-ph.CO]].
 - [10] P. Adshead and M. Wyman, *Phys. Rev. Lett.* **108**, 261302 (2012) doi:10.1103/PhysRevLett.108.261302 [[arXiv:1202.2366](#) [hep-th]].

- [11] P. Adshead and M. Wyman, Phys. Rev. D **86**, 043530 (2012) doi:10.1103/PhysRevD.86.043530 [[arXiv:1203.2264](#) [hep-th]].
- [12] P. A. R. Ade *et al.* [Planck Collaboration], Astron. Astrophys. **594**, A13 (2016) doi:10.1051/0004-6361/201525830 [[arXiv:1502.01589](#) [astro-ph.CO]].
- [13] R. R. Caldwell and E. V. Linder, Phys. Rev. Lett. **95**, 141301 (2005) doi:10.1103/PhysRevLett.95.141301 [[astro-ph/0505494](#)].
- [14] M. Doran and G. Robbers, JCAP **0606**, 026 (2006) doi:10.1088/1475-7516/2006/06/026 [[astro-ph/0601544](#)].
- [15] M. Betoule *et al.* [SDSS Collaboration], Astron. Astrophys. **568**, A22 (2014) doi:10.1051/0004-6361/201423413 [[arXiv:1401.4064](#) [astro-ph.CO]].
- [16] . Aubourg *et al.*, Phys. Rev. D **92**, no. 12, 123516 (2015) doi:10.1103/PhysRevD.92.123516 [[arXiv:1411.1074](#) [astro-ph.CO]].
- [17] G. Hinshaw *et al.* [WMAP Collaboration], Astrophys. J. Suppl. **208**, 19 (2013) doi:10.1088/0067-0049/208/2/19 [[arXiv:1212.5226](#) [astro-ph.CO]].
- [18] P. A. R. Ade *et al.* [Planck Collaboration], Astron. Astrophys. **571**, A16 (2014) doi:10.1051/0004-6361/201321591 [[arXiv:1303.5076](#) [astro-ph.CO]].
- [19] A. G. Riess *et al.*, Astrophys. J. **826**, no. 1, 56 (2016) doi:10.3847/0004-637X/826/1/56 [[arXiv:1604.01424](#) [astro-ph.CO]].
- [20] E. Di Valentino, A. Melchiorri and J. Silk, Phys. Lett. B **761**, 242 (2016) doi:10.1016/j.physletb.2016.08.043 [[arXiv:1606.00634](#) [astro-ph.CO]].
- [21] W. L. Freedman, Nat. Astron. **1**, 0169 (2017) [[arXiv:1706.02739](#) [astro-ph.CO]].
- [22] J. Bielefeld and R. R. Caldwell, Phys. Rev. D **91**, no. 12, 123501 (2015) doi:10.1103/PhysRevD.91.123501 [[arXiv:1412.6104](#) [astro-ph.CO]].
- [23] J. Bielefeld and R. R. Caldwell, Phys. Rev. D **91**, no. 12, 124004 (2015) doi:10.1103/PhysRevD.91.124004 [[arXiv:1503.05222](#) [gr-qc]].